

## VARIABLE STARS IN LARGE MAGELLANIC CLOUD GLOBULAR CLUSTERS III: RETICULUM\*

CHARLES A. KUEHN<sup>1,2</sup>, KYRA DAME<sup>1</sup>, HORACE A. SMITH<sup>1</sup>, MÁRCIO CATELAN<sup>3,4</sup>, YOUNG-BEOM JEON<sup>5</sup>, JAMES M. NEMEC<sup>6</sup>,  
 ALISTAIR R. WALKER<sup>7</sup>, ANDREA KUNDER<sup>7</sup>, BARTON J. PRITZL<sup>8</sup>, NATHAN DE LEE<sup>1,9</sup>, JURA BORISSOVA<sup>10</sup>

*Draft version February 5, 2013*

### ABSTRACT

This is the third in a series of papers studying the variable stars in old globular clusters in the Large Magellanic Cloud. The primary goal of this series is to look at how the characteristics and behavior of RR Lyrae stars in Oosterhoff-intermediate systems compare to those of their counterparts in Oosterhoff-I/II systems. In this paper we present the results of our new time-series BVI photometric study of the globular cluster Reticulum. We found a total of 32 variable stars (22 RRab, 4 RRC, and 6 RRd stars) in our field of view. We present photometric parameters and light curves for these stars. We also present physical properties, derived from Fourier analysis of light curves, for some of the RR Lyrae stars. We discuss the Oosterhoff classification of Reticulum and use our results to rederive the distance modulus and age of the cluster.

*Subject headings:* galaxies: Magellanic Clouds - stars: horizontal-branch - stars: variables: general - stars: variables: RR Lyrae

### 1. INTRODUCTION

This is the third in a series of papers focusing on the variable stars in Large Magellanic Cloud (LMC) globular clusters. The goal of this series of papers is to better understand the nature of the Oosterhoff dichotomy in the Milky Way and how Oosterhoff intermediate (Oo-int) clusters in nearby dwarf galaxies fit into that picture. Globular clusters in the Milky Way are classified as either Oosterhoff I (Oo-I) or Oosterhoff II (Oo-II) objects based on the properties of their RR Lyrae stars. Oo-I objects are defined as having an average RRab period of  $\langle P_{ab} \rangle < 0.58$  days while Oo-II objects have  $\langle P_{ab} \rangle > 0.62$  days; the typical values of  $\langle P_{ab} \rangle$  are 0.55 days and 0.65 days for Oo-I and Oo-II objects, respectively. Oo-I clusters also

tend to be more metal-rich and have a smaller ratio of first overtone dominant to fundamental mode dominant RR Lyrae. The period range between the two groups,  $0.58 \leq \langle P_{ab} \rangle \leq 0.62$  days, is referred to as the Oosterhoff gap and is essentially unoccupied by Milky Way globular clusters. The nearby dwarf galaxies and their globular clusters present a sharp contrast to this behavior as these extra-galactic clusters not only fall in the Oo-I and Oo-II groups, they also fall into the gap between these groups; in fact the extra-galactic objects seem to preferentially be located in the gap (Catelan 2009a). These Oosterhoff-intermediate objects, as objects that fall in the gap are called, present a challenge for models that propose that the Milky Way halo was formed through the accretion of objects similar to the present day nearby dwarf galaxies as we would expect to see similar Oosterhoff properties in both samples if that were the case.

The first two papers in this series discussed the variables in the globular clusters NGC 1466 (Kuehn et al. 2011) and NGC 1786 (Kuehn et al. 2012). These previous investigations, combined with the results presented here, build an inventory of updated RR Lyrae properties in a representative sample of LMC globular clusters. A future paper in the series will present a more detailed discussion of our present understanding of the Oosterhoff phenomenon and how the overall results from our study of LMC globular clusters fit into this picture.

Reticulum is an old globular cluster that is located  $\approx 11^\circ$  from the center of the LMC (Demers & Kunkel 1976). It has a metal abundance of  $[\text{Fe}/\text{H}]_{\text{ZW84}} \approx -1.66$  (Mackey & Gilmore 2004a) ( $[\text{Fe}/\text{H}]_{\text{UVES}} \approx -1.61$  in the new UVES scale (Carretta et al. 2009)) and is not very reddened,  $E(\text{B}-\text{V}) = 0.016$  (Schlegel et al. 1998). Mackey & Gilmore found that the age of Reticulum is similar to the ages of the oldest globular clusters in the Milky Way and the LMC, having an age that is approximately 1.4 Gyr younger than the classic nearby Milky Way halo globular cluster M3. Johnson et al. (2002) used Hubble Space Telescope observations to determine that Reticulum formed within 2 Gyr of the other old LMC clusters.

Reticulum is a sparsely populated cluster, but it does

\* Based on observations taken with the SMARTS 1.3-meter telescope operated by the SMARTS Consortium and observations taken at the Southern Astrophysical Research (SOAR) telescope, which is a joint project of the Ministério da Ciência, Tecnologia, e Inovação (MCTI) da República Federativa do Brasil, the U.S. National Optical Astronomy Observatory (NOAO), the University of North Carolina at Chapel Hill (UNC), and Michigan State University (MSU).

<sup>1</sup> Department of Physics and Astronomy, Michigan State University, East Lansing, MI 48824, USA; damekyra@msu.edu, smith@pa.msu.edu

<sup>2</sup> Current address: Sydney Institute for Astronomy, University of Sydney, Sydney, Australia; kuehn@physics.usyd.edu.au

<sup>3</sup> Pontificia Universidad Católica de Chile, Facultad de Física, Departamento de Astronomía y Astrofísica, Santiago, Chile; mcatelan@astro.puc.cl

<sup>4</sup> The Milky Way Millennium Nucleus, Santiago, Chile

<sup>5</sup> Korea Astronomy and Space Science Institute, Daejeon, Korea; ybjeon@kasi.re.kr

<sup>6</sup> Department of Physics and Astronomy, Camosun College, Victoria, British Columbia, Canada; nemec@camosun.bc.ca

<sup>7</sup> Cerro Tololo Inter-American Observatory, National Optical Astronomy Observatory, La Serena, Chile; awalker@ctio.noao.edu, akunder@ctio.noao.edu

<sup>8</sup> Department of Physics and Astronomy, University of Wisconsin Oshkosh, Oshkosh, WI 54901, USA; pritzlb@uwosh.edu

<sup>9</sup> Current address: Department of Physics and Astronomy, Vanderbilt University, Nashville, TN 37235, USA; nathan.delee@vanderbilt.edu

<sup>10</sup> Departamento de Física y Astronomía, Facultad de Ciencias, Universidad de Valparaíso, Valparaíso, Chile; jura.borissova@uv.cl

have a distinct horizontal branch that stretches across the instability strip (Figures 1 and 2). Twenty-two RR Lyrae stars were first found in the cluster by Demers & Kunkel (1976). Walker (1992a, hereafter Walker) later found an additional ten RR Lyrae stars, bringing the total in the cluster to 32. The pulsation types include 22 RRab stars (fundamental-mode pulsators), 9 RRC's (first-overtone), and 1 candidate RRd (double-mode pulsators), although recently Ripepi et al. (2004) found evidence for RRd behavior in four of the previously discovered RR Lyrae stars.

## 2. OBSERVATIONS AND DATA ANALYSIS

A total of 38  $V$ , 33  $B$ , and 35  $I$  images were obtained using the SOI imager (5.2x5.2 arcminute field of view) on the SOAR 4-m telescope in February of 2008. ANDICAM (6x6 arcminute field of view) on the SMARTS 1.3-m telescope operated by the SMARTS consortium was used to obtain 45  $V$ , 43  $B$ , and 45  $I$  images between September 2006 and the end of December 2006. An additional 145  $V$  and 146  $B$  image were taken with the Tek2K (13.6x13.6 arcminute field of view) on the SMARTS 0.9-m telescope between December 2008 and November 2009. SOAR exposure times were between 30s and 600s for  $V$  and  $I$ , and between 45s and 900s for  $B$ . SMARTS 1.3-m exposures were 450s for the  $V$  and  $B$  filters and 300s for the  $I$  filter. SMARTS 0.9-m exposures were 400s in both the  $V$  and  $B$ .

Data reduction and variable identification for the SOAR and SMARTS 1.3-m data were carried out as described in Kuehn et al. (2011), the same method used for both NGC 1466 and NGC 1786. The SMARTS 0.9-m data was processed using the method described in Jeon et al. (2012). The uncrowded nature of Reticulum was ideal for Daophot's profile fitting photometry (Stetson 1987, 1992, 1994) and while an image differencing method (ISIS; Alard 2000) was run on the images for completeness, no additional variable stars were recovered. The photometry from Daophot was transformed to the standard system using the Landolt standard fields PG0231, SA95, and SA98 (Landolt 1992). We compared our resulting photometry to five of the local standard stars used by Walker, finding that for these five stars our photometry was  $0.011 \pm 0.010$  magnitudes brighter in  $V$  and  $0.001 \pm 0.018$  in  $B$ .

## 3. VARIABLE STARS

All 32 RR Lyrae stars first found by Walker were recovered: 22 RRab stars, 4 RRC's, and 6 RRd's. The 6 RRd stars were originally classified as RRC stars by Walker but the larger number of observations in our data set allowed for the identification of secondary pulsation modes. The RRab and RRC stars and their observed characteristics (periods,  $V$ ,  $B$ , and  $I$  amplitudes, intensity-weighted  $V$ ,  $B$ , and  $I$  mean magnitudes, and magnitude-weighted mean  $B-V$  color) are listed in Table 1; the stars that potentially show the Blazhko effect are identified with 'BL' after their name. The RRd stars, their fundamental and first overtone periods and amplitudes, their period ratios, and their mean magnitudes and color are listed in Table 2. Periods for RRab and RRC stars are typically good to  $\pm 0.00001$  or  $\pm 0.00002$  days while periods for RRd stars are less well known, with uncertainties about an order of magnitude larger. Walker identified the variables in

this paper using their star number in the catalog compiled in Demers & Kunkel (1976). We introduce a new naming system that features only the variable stars and is ordered based on increasing RA. The names used by Walker are listed in the last column in Tables 1 and 2. Table 3 gives the photometry for the RR Lyrae stars and Figures 3, 4, and 5 show the light curves for the RRab, RRC, and RRd stars, respectively. The positions of the variable stars within the cluster are shown in Figure 6.

The RRab stars have intensity-weighted mean magnitudes of  $\langle V \rangle = 19.06 \pm 0.01$ ,  $\langle B \rangle = 19.39 \pm 0.01$ , and  $\langle I \rangle = 18.61 \pm 0.01$  while the RRC stars have mean magnitudes of  $\langle V \rangle = 19.05 \pm 0.02$ ,  $\langle B \rangle = 19.26 \pm 0.04$ , and  $\langle I \rangle = 18.69 \pm 0.01$ . The results for RRab stars are 0.02 mag brighter than the mean magnitudes found by Walker while our values for the RRC stars are consistent within the errors of those found by Walker.

In general our periods agreed with those of Walker to within 0.0002 days. V08 and V19 were the only stars for which a difference in period greater than 0.01 days was found. Walker found a period of 0.6566 days for V08 while we found a period of 0.64495 days, a decrease of 0.0117 days. For V19, Walker found a period of 0.469 days while we found a period of 0.48485 days, an increase of 0.016days. We believe the periods adopted represent these stars more accurately, as our phase coverage is significantly more complete than that of Walker.

The first overtone periods for the RRd stars show good agreement with the periods that Walker had reported. Four of the six RRd stars (V03, V11, V15, V24) were also found by Ripepi et al. (2004). Figure 7 shows the Petersen diagram for the RRd stars in Reticulum along with those in the field of the LMC. The Reticulum RRd stars have similar period ratios to not only the LMC field RRd stars, but also to the RRd stars found in Milky Way Oo-I clusters (Clementini et al. 2004). The right hand panel shows the results for models from Bragaglia et al. (2001) for three different combinations of metallicity, mass, and luminosity of the RRd stars. The RRd stars in Reticulum are fit very well by the line that corresponds to a metallicity of  $[\text{Fe}/\text{H}]_{\text{ZW84}} = -1.53$  ( $[\text{Fe}/\text{H}]_{\text{UVES}} = -1.45$ ), a mass of  $M/M_{\odot} = 0.80$ , and a luminosity of  $\log(L/L_{\odot}) = 1.72$ . However, this gives a mass that is much higher than the masses of the RRC stars calculated through the Fourier decomposition method (see §4) or from fitting horizontal branch evolutionary tracks to the color-magnitude diagram (§5). The model tracks for a metallicity of  $[\text{Fe}/\text{H}]_{\text{ZW84}} = -1.71$  ( $[\text{Fe}/\text{H}]_{\text{UVES}} = -1.68$ ) suggests that the Reticulum RRd stars could also be fit by a model of that metallicity with a mass in the range of  $0.70 < M/M_{\odot} < 0.75$  which would be closer to the masses obtained for the RRC stars.

## 4. PHYSICAL PROPERTIES OF THE RR LYRAE STARS

It has been shown that the Fourier parameters of RR Lyrae light curves can be used to estimate their physical properties (e.g., Jurcsik & Kovacs 1996, Jurcsik 1998, Simon & Clement 1993). The RRab light curves were fit with a Fourier series of the form

$$m(t) = A_0 + \sum_{j=1}^n A_j \sin(j\omega t + \phi_j), \quad (1)$$

while the RRc light curves were fit with a cosine series. The resulting Fourier coefficients were then used to calculate physical properties of the stars using the relations from Jurcsik & Kovács (1996), Jurcsik (1998), Kovács & Walker (1999, 2001), Simon & Clement (1993), and Morgan, Wahl, & Wieckhorst (2007). We refer the reader to the first paper in this series, Kuehn et al. (2011), for further details.

Although a Fourier decomposition was attempted on all the RRab and RRc stars, only 14 RRab and 3 RRc had light curves that allowed the reliable determination of Fourier parameters. Tables 4 and 5 give the Fourier coefficients for the RRab and RRc stars, respectively. The physical properties determined from these coefficients are given in Tables 6 and 7. Table 4 also lists the Jurcsik & Kovács  $D_{max}$  values (Jurcsik & Kovács 1996) for the RRab stars.  $D_{max}$  can be used to separate RRab stars with “regular” light curves from those with more “anomalous” light curves; lower values represent more regular light curves. Jurcsik & Kovács (1996) suggest that stars with  $D_{max} > 3$  should not be trusted to provide reliable physical properties. We take a slightly more liberal approach and use the RRab stars with  $D_{max} < 5$  to determine the average properties for the cluster; following the condition from Jurcsik & Kovács does not change the average values by a significant amount.

The mean metallicity of the RRab stars is  $[\text{Fe}/\text{H}]_{J95} = -1.43 \pm 0.02$  which is  $[\text{Fe}/\text{H}]_{ZW84} = -1.61 \pm 0.02$  on the Zinn & West scale and  $[\text{Fe}/\text{H}]_{UVES} = -1.55 \pm 0.04$ . This value is similar to the metallicity of  $[\text{Fe}/\text{H}]_{UVES} \simeq -1.61$  found by Mackey & Gilmore (2004a). On the other hand, the relation from Morgan, Wahl, & Wieckhorst (2007) gives a metallicity for the RRc stars of  $[\text{Fe}/\text{H}]_{ZW84} = -1.75 \pm 0.03$ ,  $[\text{Fe}/\text{H}]_{UVES} = -1.73 \pm 0.06$ , which is more metal-poor than the values obtained from the RRab stars and the literature, but still within the 0.2 dex error estimation in their empirical relation. While this difference in metallicity could be caused by errors in the Fourier analysis, the fact that the other physical properties obtained for the RRc stars are consistent with expectations lends support to the validity of the obtained Fourier coefficients.

## 5. DISTANCE MODULUS

The absolute magnitude-metallicity relationship from Catelan & Cortés (2008) is used to provide the absolute magnitude of the RR Lyrae stars in Reticulum. The disagreement between the metallicities for RRab and RRc stars raises an issue as to which metallicity to use for calculating the absolute magnitude. Since the metallicity obtained from the RRab stars is consistent with what has been reported in the literature and is drawn from a larger number of stars, that value is used,  $[\text{Fe}/\text{H}]_{ZW84} = -1.61 \pm 0.02$ . This value gives an absolute magnitude of  $M_V = 0.61 \pm 0.20$ . The average magnitude of the RRab stars,  $\langle V \rangle = 19.064 \pm 0.008$ , and the reddening value of  $E(B-V) = 0.016$  from Schlegel et al. (1998) are used, along with a standard extinction law of  $A_V/E(B-V) = 3.1$ , to obtain a reddening-corrected distance modulus of  $(m-M)_0 = 18.40 \pm 0.20$ , which agrees with the value of  $18.39 \pm 0.12$  found by Ripepi et al. (2004). This is shorter than the distance modulus of  $(m-M)_{LMC} = 18.44 \pm 0.11$  that Catelan & Cortés (2008) derived for the LMC, though the two distance

moduli agree within the errors. This is not necessarily a surprise as Reticulum is widely separated from the disk of the LMC, having a location that is about 11 degrees from the center of the LMC (Walker 1992a).

Despite the changes in color during the pulsation cycle of an RR Lyrae stars, RRab stars show a very small range of intrinsic  $V-I$  color during their minimum light phase (Mateo et al. 1995). We compare the  $V-I$  colors of our RRab stars to the expected color of  $(V-I)_{0,min} = 0.58 \pm 0.02$  from Guldenschuh et al. (2005); Table 8 lists the  $(V-I)_{min}$  colors and the reddening,  $E(V-I)$  for each of the RRab stars in Reticulum. The average reddening from the RRab stars is  $E(V-I) = -0.01 \pm 0.02$ ; this is less than the reddening value of  $E(V-I) = 0.026$  that is expected based on the  $E(B-V) = 0.016$  from Schlegel et al. (1998).

## 6. THE CMD

Our color-magnitude diagram (CMD) is compared to theoretical isochrones from the Princeton-Goddard-PUC (PGPUC) stellar evolutionary code (Valcarce et al. 2012). The RR Lyrae distance modulus of  $(m-M)_V = 18.45$  mag is adopted; assuming a reddening of  $E(B-V) = 0.016$  Schlegel et al. (1998), the true distance modulus is  $(m-M)_{V,0} = 18.40$  mag, as discussed in §5. Although there have been some suggestions that the reddening towards Reticulum is larger than that adopted here (e.g., Mackey & Gilmore 2004), as shown below, no evidence is found to support a larger reddening value than reported by Schlegel et al. (1998); the reddening value obtained from the  $V-I$  colors of the RRab stars at minimum light also do not support a larger reddening value. Isochrones with a “normal”  $[\alpha/\text{Fe}]$  ratio (e.g., Mateluna et al. 2012),  $Y = 0.245$  and  $Z = 0.0006$  (corresponding to  $[\text{Fe}/\text{H}]_{UVES} \sim -1.61$  dex) are over-plotted.

Figure 8 shows that the best fit isochrones have ages of  $\sim 14 \pm 2$  Gyr, consistent with the ages of other LMC GCs (Olsen 1999, Mackey & Gilmore 2004, Bekki et al. 2008). The observed RGB fits the CMD well. In contrast, a larger reddening value would shift the isochrones to the red. A smaller  $[\alpha/\text{Fe}]$  or a more metal-poor  $[\text{Fe}/\text{H}]$  would shift the isochrones to the blue, as would a smaller reddening value. We therefore see no need to adopt a larger value of reddening than that found by Schlegel et al. (1998). A small reddening value is also in agreement with the  $E(B-V) = 0.03$  derived by Walker (1992a). We believe Figure 8 provides evidence that our derived RR Lyrae distance modulus fits the CMD remarkably well and supports an old age of Reticulum.

Figure 9 shows the  $V, (V-I)$  CMD for Reticulum centered on the RR Lyrae instability strip. A Zero Age Horizontal Branch (ZAHB) from the BaSTI HB tracks (Pietrinferni et al. 2004, 2006) with  $Z = 0.0006$  is over-plotted, as well as the BaSTI evolutionary tracks for  $0.65 M_\odot$ , to  $0.68 M_\odot$  HB stars. As shown by Gallart et al. 2005, the deviation of the mean RR Lyrae magnitudes from the ZAHB is  $\delta(V_{ZAHB} - \langle V \rangle)_{RR} \sim 0.1$  mag at the metallicity of Reticulum, and hence we adopt  $(m-M)_{V0,ZAHB} = 18.50$  mag. The BaSTI tracks indicate that most of the Reticulum RR Lyrae stars have a mass range of  $0.65 - 0.68 M_\odot$ . These RR Lyrae masses are a little larger than those found from the Fourier decomposition of the RRc stars (see Table 5), although the mass of V28 derived from the BaSTI tracks and from the

Fourier decomposition technique agrees remarkably well. We note that changing  $(m - M)_{V0,ZAHB}$  does not affect the derived RR Lyrae masses. In contrast, a change in  $Z$  affects the theoretical RR Lyrae masses in a sense that a more metal-rich  $Z$  shifts the RR Lyrae masses to smaller values.

## 7. OOSTERHOFF CLASSIFICATION

The average periods for the RR Lyrae stars in Reticulum are  $\langle P_{ab} \rangle = 0.552$  days and  $\langle P_c \rangle = 0.325$  days. The 22 RRab stars, 4 RRc's, and 6 RRd's give the cluster a number fraction of  $N_{c+d}/N_{c+d+ab} = 0.31$ . The average periods for the RRab and RRc stars strongly indicate an Oosterhoff I classification and, while the number fraction is high, it is still consistent with the cluster being an Oo-I object. The minimum period for an RRab star in Reticulum is  $P_{ab,min} = 0.46862$  days, which is also consistent with an Oo-I classification for Reticulum Catelan et al. (2012).

Figure 10 shows the  $V$  and  $B$  band period-amplitude diagrams for Reticulum. Both diagrams show that the RRab stars cluster along the line that indicates the typical location for RRab stars in Oo-I clusters. There is more scatter in the positions of the RRc stars but most of them still are located near the Oo-I locus, confirming the classification of Reticulum as an Oo-I object.

## 8. CONCLUSION

We have conducted a photometric study of the Reticulum globular cluster in order to identify and classify the variable stars in that cluster; our data set consists of 228  $V$ , 222  $B$ , and 80  $I$  images, making it the largest such data set on Reticulum. We found a total of 32 RR Lyrae stars (22 RRab, 4 RRc, and 6 RRd) in the cluster. While all 32 stars had been previously discovered, we were able to discover secondary pulsation periods in 2 stars that had previously been classified as RRc stars.

We calculated Fourier parameters for a sub-sample of the RRab and RRc stars and used these to determine the physical properties of the RR Lyrae stars in Reticulum for the first time. A future paper in this series will compare these physical properties to those obtained for other clusters in order to look at the differences between clusters of different Oosterhoff type.

The  $V$ ,  $(V - I)$  CMD of the cluster was used to calculate an age of  $\sim 14 \pm 2$  Gyr for Reticulum, consistent with the age of the other old globular clusters in the LMC.

The average periods for the RRab and RRc stars indicate that Reticulum is an Oosterhoff I cluster. This is confirmed by the location of the RRab and RRc stars on the Bailey diagram and the location of the RRd stars on the Petersen diagram.

## 9. ACKNOWLEDGEMENTS

Support for H.A.S. and C.A.K. is provided by NSF grants AST 0607249 and AST 0707756.

## REFERENCES

- Alard, C. 2000, *A&AS*, 144, 363  
 Bekki, K., Yahagi, H., Nagashima, M., & Forbes, D.A. 2008, *MNRAS*, 387, 1131  
 Bragaglia, A., et al. 2001, *AJ*, 122, 207  
 Cacciari, C., Corwin, T. M., & Carney, B.W. 2005, *AJ*, 129, 267  
 Carretta, E. et al. 2009, *A&A*, 508, 695  
 Carretta, E., & Gratton, R.G. 1997, *A&AS*, 121, 95  
 Catelan, M. 2009a, *Ap&SS*, 320, 261  
 Catelan, M., & Cortés, C. 2008, *ApJ*, 676, L135  
 Catelan, M., et al. 2012, *AJ*, submitted  
 Clementini, G., Corwin, T.M., Carney, B.W., & Sumerel, A.N. 2004, *AJ*, 127, 938  
 Demers, S. & Kunkel, W.E. 1976, *ApJ*, 208, 932  
 Gallart, C., Zoccali, M., & Aparicio, A. 2005, *ARA&A*, 43, 387  
 Guldenschuh, K.A. et al. 2005, *PASP*, 117, 721  
 Jeon, Y.B., Nemeč, J.M., Walker, A.R., & Kunder, A.M. 2012, *JKAS*, 45, 125  
 Johnson, J.A., Bolte, M., Stetson, P.B., & Hesser, J.E. 2002, *IAU Symp.* 207, 190  
 Jurcsik, J. 1995, *AcA*, 45, 653  
 Jurcsik, J. 1998, *A&A*, 333, 571  
 Jurcsik, J., & Kovács, G. 1996, *A&A*, 312, 111  
 Kovács, G., & Walker, A.R. 1999, *ApJ*, 512, 271  
 Kovács, G., & Walker, A.R. 2001, *A&A*, 371, 579  
 Kuehn, C.A. et al. 2011, *AJ*, 142, 107  
 Kuehn, C.A. et al. 2012, *AJ*, 144, 186  
 Kunder, A., Stetson, P.B., Catelan, M., Walker, A.R., Amigo, P. 2013, *AJ*, 145, 33  
 Landolt, A.U. 1992, *AJ*, 104, 340  
 Mackey, A.D., & Gilmore, G.F. 2004, *MNRAS*, 352, 153  
 Mateluna, R. et al. 2012, *A&A*, 548, 82  
 Mateo, M. et al. 1995, *AJ*, 109, 588  
 Morgan, S.M., Wahl, J.N., & Wieckhorst, R.M. 2007, *MNRAS*, 374, 1421  
 Olsen, K.A.G. 1999, *AJ*, 117, 2244  
 Pietrinferni, A., Cassisi, S., Salaris, M., & Castelli, F. 2004, *ApJ*, 612, 168  
 Pietrinferni, A., Cassisi, S., Salaris, M., & Castelli, F. 2007, *ApJ*, 642, 797  
 Ripepi, V. et al. 2004, *CoAst.*, 145, 24  
 Schlegel, D.J., Finkbeiner, D.P., & Davis, M. 1998, *ApJ*, 500, 525  
 Simon, N.R., & Clement, C.M. 1993, *ApJ*, 410, 526  
 Soszyński, I., et al. 2003, *AcA*, 53, 93  
 Stetson, P.B. 1987, *PASP*, 99, 191  
 Stetson, P.B. 1992, in *ASP Conf. Ser.* 25, *Astronomical Data Analysis Software and Systems I*, ed. D.M. Worrall, C. Biemesderfer, & J. Barnes (San Francisco: ASP), 297  
 Stetson, P.B. 1994, *PASP*, 106, 250  
 Valcarce, A.A.R., Catelan, M., Sweigart, A.V. 2012, *A&A*, 547, 5  
 Walker, A.R. 1992, *AJ*, 103, 1166  
 Zinn, R., & West, M.J. 1984, *ApJS*, 55, 45  
 Zorotovic, M., et al. 2010, *AJ*, 139, 357; erratum: 2010, *AJ*, 140, 912

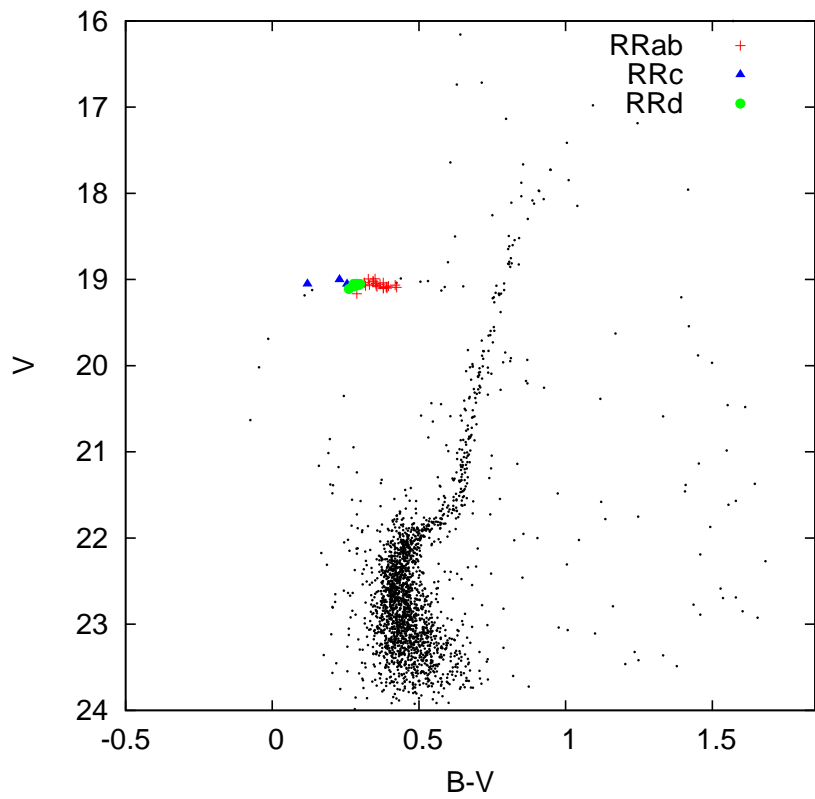


**Figure 1.**  $V, B - V$  CMD for Reticulum with the position of the RR Lyrae variables also indicated. Plus symbols indicate RRab stars, filled triangles indicated RRc's, and circles indicate RRd's.

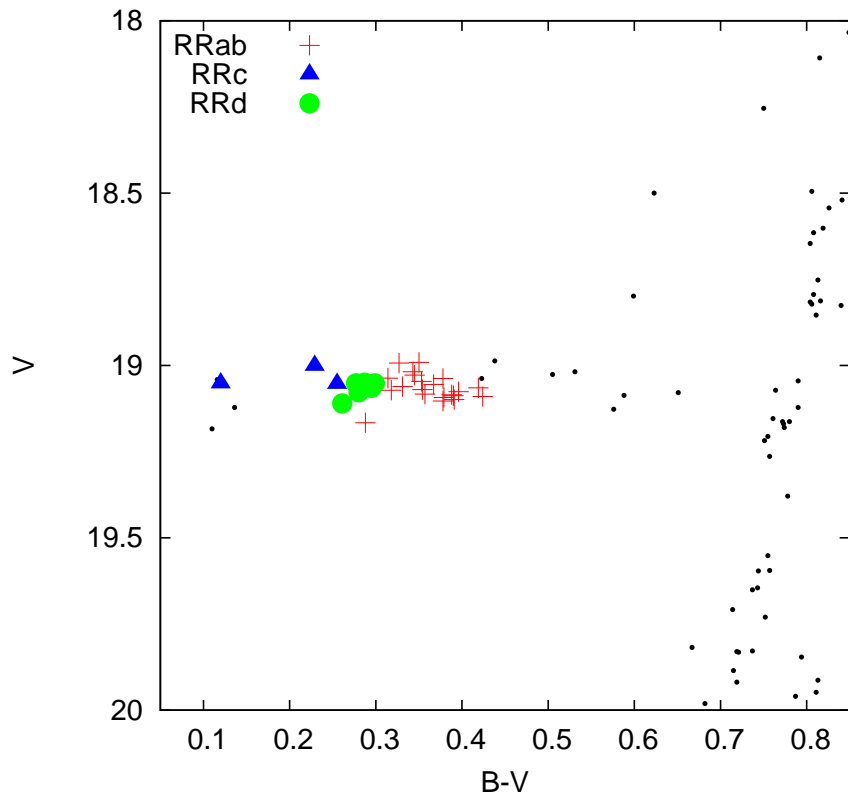


**Figure 2.**  $V, B - V$  CMD for Reticulum that is zoomed in on the horizontal branch. The symbols used are the same as in Figure 1

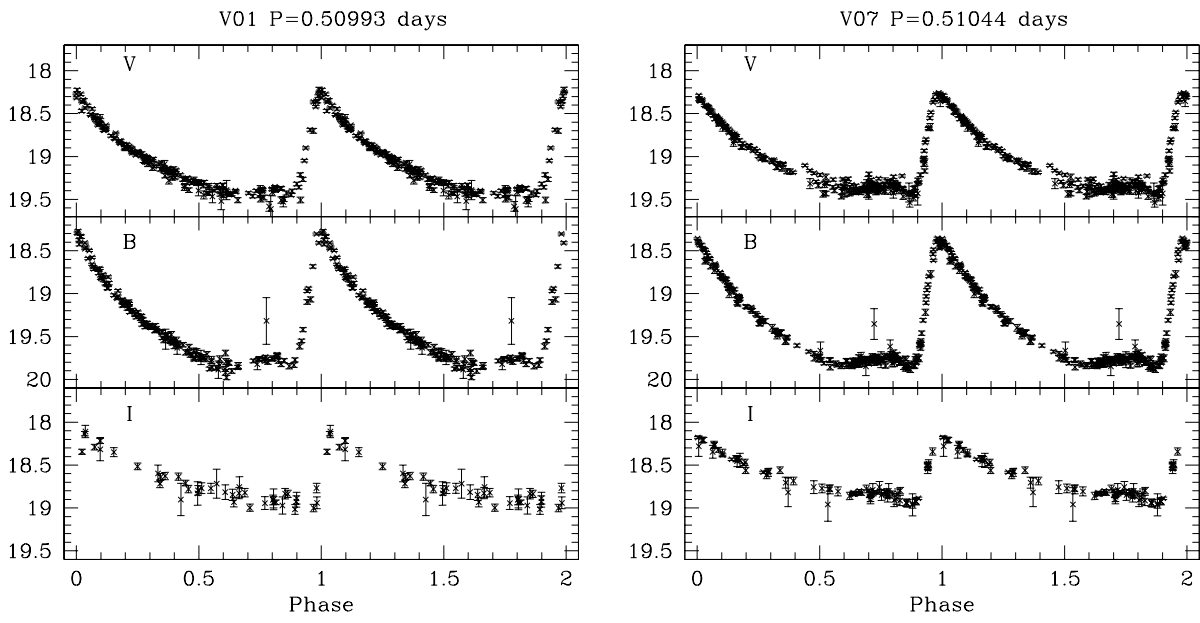


**Figure 3.** Sample light curves for R Rab stars in Reticulum, the full set of light curves can be found in the electronic version of this paper.

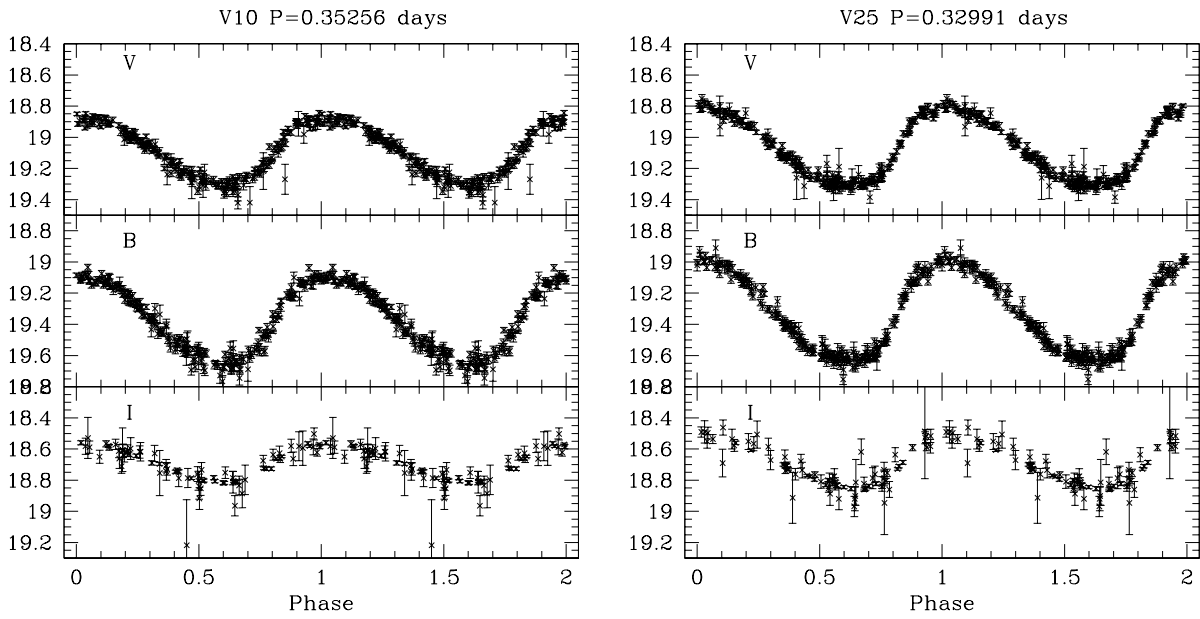


**Figure 4.** Sample light curves for R Rc stars in Reticulum, the full set of light curves can be found in the electronic version of this paper.

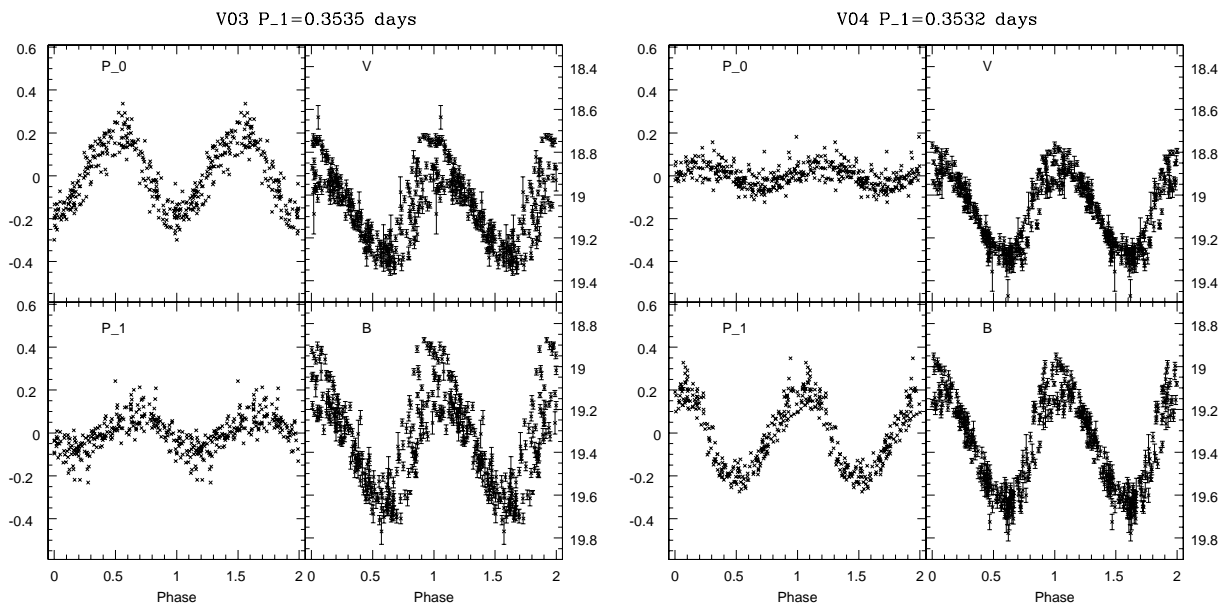


**Figure 5.** Sample light curves for RRd stars in Reticulum. The left panels show the residuals in the *V*-band light curves left from subtracting the fundamental or first overtone periods. The right panels show the *V* and *B*-band light curves plotted with the first overtone periods. The full set of light curves can be found in the electronic version of this paper.

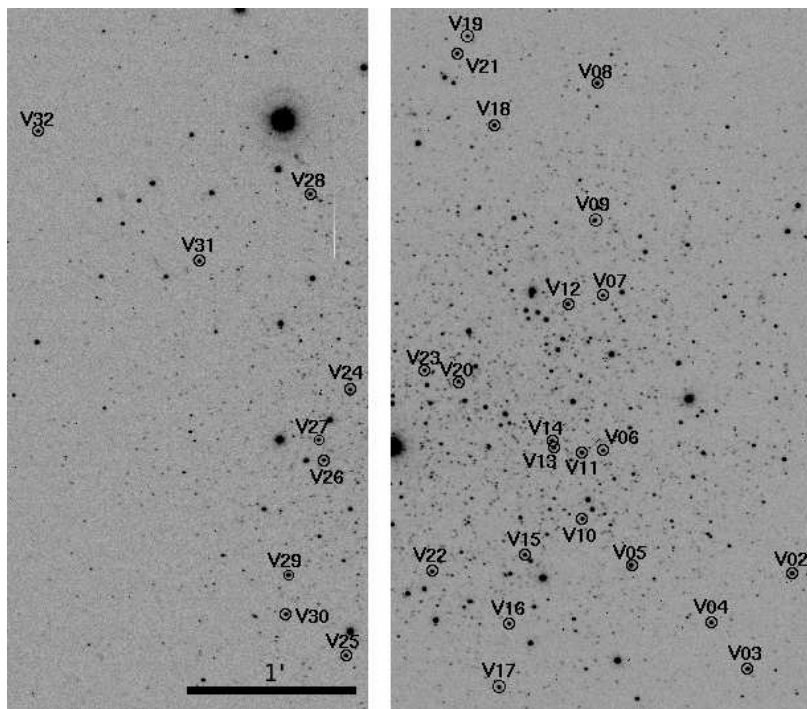


**Figure 6.** Finding chart for the variable stars in Reticulum. North is up and East is to the left. The white gap is due to the finding chart being made from a SOAR image and represents the 7.8 arcsec mounting gap between the two CCDs of the SOI camera.

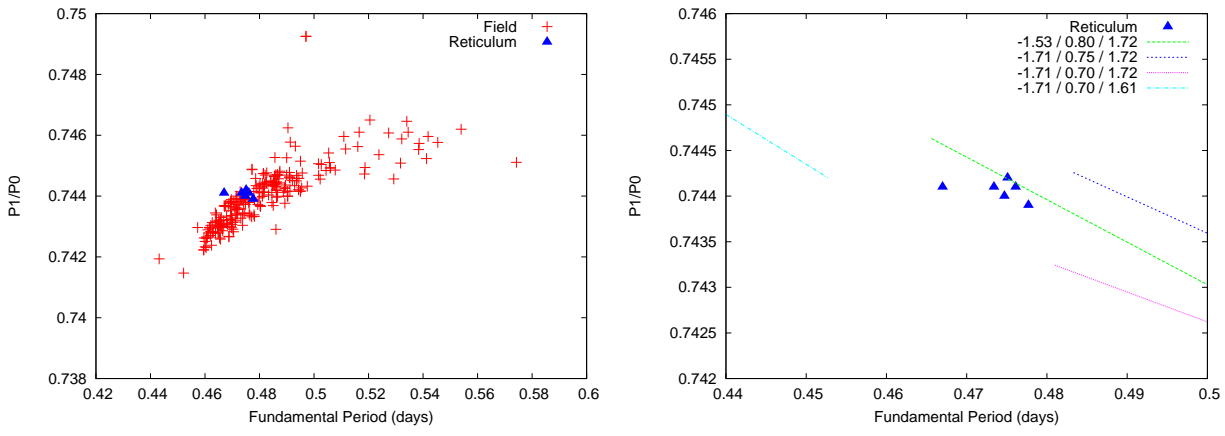


**Figure 7.** Petersen diagram showing the ratio of the first overtone period to the fundamental mode period vs. fundamental mode period for the RRd stars in Reticulum (blue triangles). (Left panel) The RRd stars in the LMC field (red plus symbols) from Soszyński et al. (2003) are also plotted. (Right panel) The colored lines are from the models by Bragaglia et al. (2001); their labels indicate the assumed metallicity ( $[Fe/H]_{ZW84}$ ), mass ratio ( $M/M_{\odot}$ ), and luminosity ( $\log(L/L_{\odot})$ ).

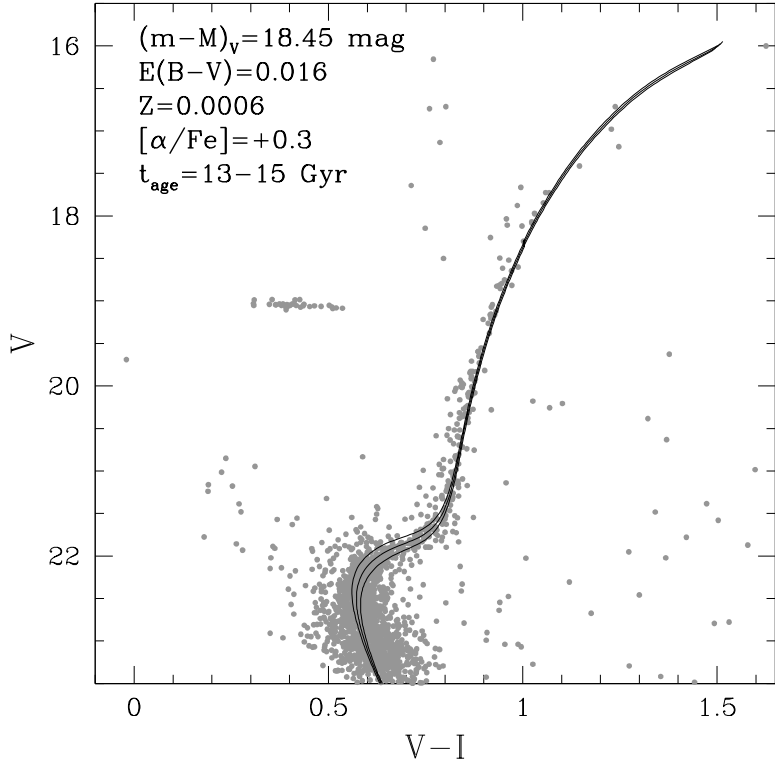


**Figure 8.** The  $V, (V - I)$  CMD for Reticulum with theoretical isochrones from the Princeton-Goddard-PUC stellar evolutionary code (Valcarce et al. 2012) also plotted. The isochrones fit the observed RGB well and suggest an age of  $\sim 14$  Gyr for Reticulum.

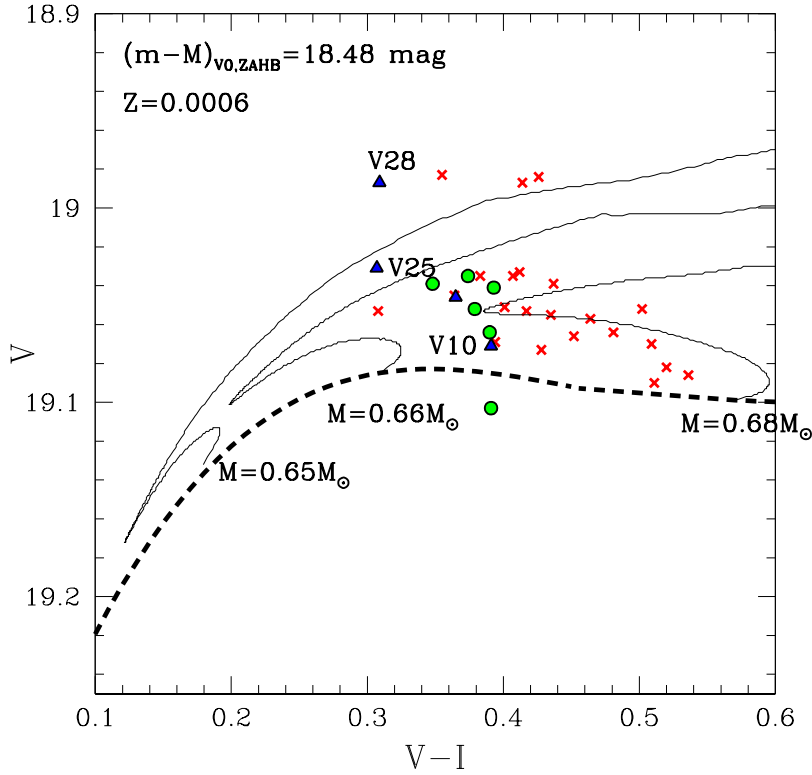


**Figure 9.** The  $V,(V-I)$  CMD for Reticulum centered on the RR Lyrae instability strip. A Zero Age Horizontal Branch from the BaSTI HB tracks (Pietrinferni et al. 2004, 2006) with  $Z=0.0006$  is overplotted, as well as the BaSTI evolutionary tracks for  $0.65M_{\odot}$ , to  $0.68M_{\odot}$  HB stars. RRab stars are indicated by red X's, RRc stars by blue triangles, and RRd stars by green circles.

**Table 1**  
Photometric Parameters for Variables in Reticulum

ID	RA (J2000)	DEC (J2000)	Type	$P$ (days)	$A_V$	$A_B$	$A_I$	$\langle V \rangle$	$\langle B \rangle$	$\langle I \rangle$	$\langle B - V \rangle$	Other IDs
V01	04:35:51.4	-58:51:03.4	RRab	0.50993	1.21	1.62	0.85	19.037	19.299	18.651	0.314	DK92
V02	04:35:56.5	-58:52:32.0	RRab	0.61869	0.66	0.91	0.44	19.085	19.455	18.561	0.388	DK7
V05	04:36:04.1	-58:52:29.4	RRab	0.57185	0.94	1.28	0.55	19.038	19.386	18.606	0.378	DK80
V06-BL	04:36:05.4	-58:51:48.0	RRab	0.59526	0.84	1.10	0.58	19.099	19.476	18.583	0.391	DK97
V07	04:36:05.5	-58:50:51.9	RRab	0.51044	1.18	1.56	0.75	18.991	19.298	18.638	0.350	DK117
V08	04:36:05.8	-58:49:35.1	RRab	0.64496	0.45	0.59	0.26	19.065	19.475	18.550	0.419	DK135
V09	04:36:05.9	-58:50:24.6	RRab	0.54496	0.92	1.08	0.45	18.993	19.295	18.589	0.327	DK137
V10	04:36:06.4	-58:52:12.8	RRc	0.35256	0.43	0.56	0.25	19.075	19.358	18.685	0.290	DK77
V12	04:36:07.1	-58:50:55.0	RRc	0.29627	0.25	0.31	0.15	19.052	19.169	18.724	0.120	DK181
V13	04:36:07.7	-58:51:47.0	RRab	0.60958	0.75	0.94	0.48	19.103	19.462	18.580	0.378	DK99
V14-BL	04:36:07.8	-58:51:44.6	RRab	0.58661	0.74	0.94	0.51	19.076	19.451	18.594	0.396	DK100
V16	04:36:09.8	-58:52:50.8	RRab	0.52290	1.21	1.61	0.79	19.046	19.351	18.629	0.353	DK49
V17	04:36:10.2	-58:53:13.7	RRab	0.51241	1.15	1.45	0.70	19.028	19.325	18.650	0.345	DK38
V18	04:36:10.6	-58:49:50.4	RRab	0.56005	1.00	1.34	0.61	19.083	19.405	18.615	0.357	DK142
V19	04:36:11.9	-58:49:18.2	RRab	0.48485	1.32	1.73	0.78	19.057	19.303	18.682	0.298	DK146
V20-BL	04:36:12.2	-58:51:23.3	RRab	0.56075	1.03	1.36	0.59	19.088	19.455	18.645	0.390	DK112
V21	04:36:12.3	-58:49:24.5	RRab	0.60700	0.72	0.95	0.52	19.093	19.452	18.564	0.379	DK145
V22	04:36:13.4	-58:52:32.1	RRab	0.51359	0.97	1.21	0.58	19.072	19.355	18.620	0.318	DK57
V23-BL	04:36:13.8	-58:51:19.3	RRab	0.46863	0.96	1.30	0.59	19.166	19.415	18.740	0.288	DK108
V25	04:36:17.4	-58:53:02.7	RRc	0.32991	0.52	0.67	0.33	19.053	19.297	18.681	0.255	DK36
V26	04:36:18.5	-58:51:52.0	RRab	0.65696	0.34	0.46	0.22	19.090	19.509	18.424	0.424	DK67
V27	04:36:18.7	-58:51:44.6	RRab	0.51382	1.25	1.64	0.79	19.055	19.374	18.637	0.367	DK64
V28	04:36:19.2	-58:50:15.7	RRc	0.31994	0.51	0.66	0.32	19.001	19.219	18.679	0.229	DK151
V29	04:36:20.1	-58:52:33.6	RRab	0.50815	1.21	1.58	0.80	19.061	19.338	18.640	0.331	DK37
V30	04:36:20.2	-58:52:47.7	RRab	0.53501	1.16	1.52	0.72	19.018	19.318	18.577	0.343	DK35
V31	04:36:24.4	-58:50:40.1	RRab	0.50516	1.11	1.52	0.67	19.070	19.379	18.681	0.354	DK25

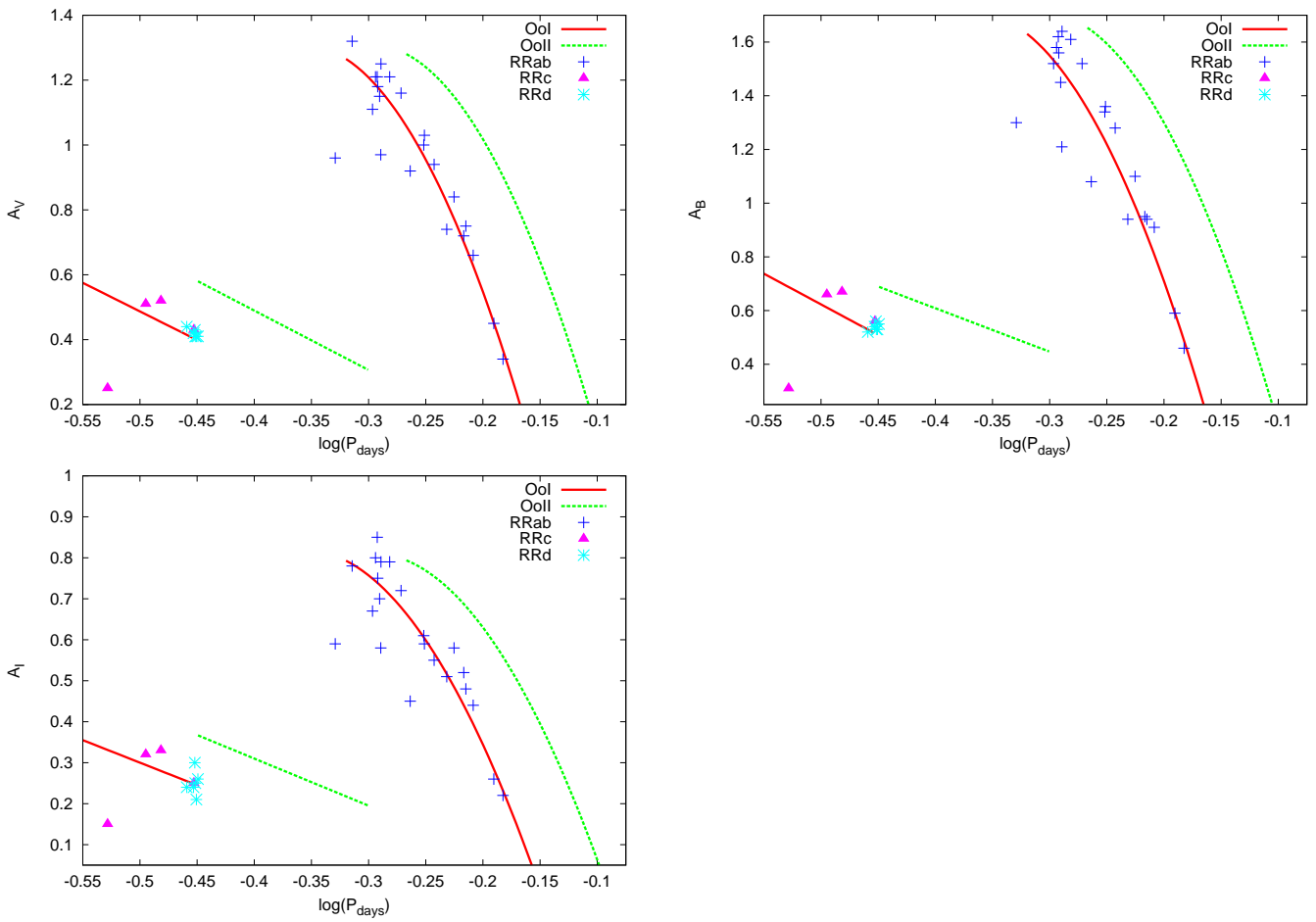


**Figure 10.** Bailey diagrams, log period vs  $V$ -band (top left),  $B$ -band (top right),  $I$ -band (bottom) amplitude for the RR Lyrae stars in Reticulum. Red and green lines indicate the typical position for RR Lyrae stars in Oosterhoff I and Oosterhoff II clusters, respectively (Cacciari et al. 2005; Zorotovic et al. 2010; Kunder et al. 2013).

**Table 2**  
Photometric Parameters for the RRD Variables in Reticulum

ID	RA (J2000)	DEC (J2000)	$P_0$ (d)	$P_1$ (d)	$P_1/P_0$	$A_{V,0}$	$A_{V,1}$	$A_{B,0}$	$A_{B,1}$	$A_{I,0}$	$A_{I,1}$	$\langle V \rangle$	$\langle B \rangle$	$\langle I \rangle$	$\langle B - V \rangle$	Oth
V03	04:35:58.6	-58:53:06.7	0.4751	0.3535	0.7442	0.21	0.41	0.25	0.53	0.13	0.25	19.050	19.329	18.662	0.287	D
V04	04:36:00.3	-58:52:50.0	0.4747	0.3532	0.7440	0.12	0.43	0.13	0.56	0.13	0.30	19.065	19.351	18.674	0.295	I
V11	04:36:06.4	-58:51:48.7	0.4777	0.3554	0.7439	0.32	0.41	0.44	0.55	0.23	0.26	19.052	19.341	18.693	0.299	D
V15	04:36:09.1	-58:52:25.9	0.4761	0.3543	0.7441	0.28	0.41	0.38	0.53	0.19	0.21	19.110	19.364	18.721	0.261	D
V24	04:36:17.3	-58:51:26.3	0.4670	0.3475	0.7441	0.27	0.44	0.26	0.52	0.17	0.24	19.078	19.350	18.673	0.280	D
V32	04:36:31.9	-58:49:53.2	0.4734	0.3523	0.7441	0.12	0.42	0.10	0.54	0.05	0.24	19.052	19.322	18.649	0.277	D

**Table 3**  
Photometry of the Variable Stars

ID	Filter	JD	Mag	Mag Error	Phase
V01	V	2453986.7538	18.556	0.044	0.09686
V01	V	2453990.7673	18.700	0.028	1.96747
V01	V	2453993.8053	19.267	0.024	0.92510
V01	V	2453995.8001	19.508	0.037	1.83697
V01	V	2453999.7524	19.438	0.024	1.58757

**Note.** — Maximum light occurs at a phase of 0. This table is published in its entirety in the electronic edition.

**Table 4**  
Fourier Coefficients for RRAb Variables

ID	$A_1$	$A_{21}$	$A_{31}$	$A_{41}$	$\phi_{21}$	$\phi_{31}$	$\phi_{41}$	$D_{max}$	Order
V02	0.243	0.455	0.306	0.166	2.469	5.152±0.051	1.817	2.0	7
V05	0.320	0.460	0.338	0.235	2.315	4.972±0.043	1.356	1.6	7
V13	0.267	0.462	0.330	0.204	2.375	5.130±0.053	1.632	3.6	7
V18	0.339	0.453	0.359	0.227	2.286	4.884±0.045	1.349	4.3	8
V21	0.259	0.453	0.325	0.209	2.438	5.166±0.075	1.772	3.2	9
V07	0.404	0.457	0.330	0.248	2.234	4.694±0.056	0.933	42.1	8
V14	0.273	0.449	0.336	0.208	2.373	4.940±0.091	1.334	46.4	8
V16	0.416	0.426	0.324	0.237	2.273	4.777±0.041	1.090	44.0	9
V17	0.390	0.425	0.330	0.207	2.191	4.625±0.056	1.027	44.5	7
V22	0.349	0.443	0.308	0.155	2.332	4.754±0.062	1.075	40.6	8
V27	0.433	0.446	0.352	0.224	2.277	4.700±0.036	1.061	45.4	9
V29	0.416	0.468	0.325	0.221	2.217	4.676±0.045	0.993	43.8	8
V30	0.400	0.447	0.323	0.196	2.308	4.922±0.063	1.151	40.9	8
V31	0.400	0.428	0.335	0.208	2.237	4.755±0.044	1.007	43.0	8

**Table 5**  
Fourier Coefficients for RRc Variables

ID	$A_1$	$A_{21}$	$A_{31}$	$A_{41}$	$\phi_{21}$	$\phi_{31}$	$\phi_{41}$	Order
V10	0.219	0.134	0.076	0.031	4.878	3.467±0.207	2.244	6
V25	0.247	0.135	0.086	0.045	4.822	3.258±0.143	1.715	7
V28	0.245	0.170	0.097	0.034	4.712	3.023±0.224	0.898	6

**Table 6**  
Derived Physical Properties for RRAb Variables

ID	$[\text{Fe}/\text{H}]_{\text{J95}}$	$\langle M_V \rangle$	$\langle V - K \rangle$	$\log T_{\text{eff}}^{(V-K)}$	$\langle B - V \rangle$	$\log T_{\text{eff}}^{(B-V)}$	$\langle V - I \rangle$	$\log T_{\text{eff}}^{(V-I)}$	$\log g$
V02	-1.446	0.772	1.204	3.800	0.366	3.802	0.528	3.801	2.740
V05	-1.435	0.782	1.137	3.807	0.346	3.809	0.502	3.808	2.780
V13	-1.427	0.771	1.179	3.803	0.362	3.804	0.522	3.803	2.747
V18	-1.490	0.780	1.137	3.807	0.342	3.810	0.497	3.810	2.791
V21	-1.363	0.782	1.178	3.802	0.363	3.804	0.523	3.803	2.749
V07	-1.478	0.799	1.076	3.814	0.317	3.819	0.466	3.818	2.840
V14	-1.557	0.781	1.175	3.803	0.358	3.804	0.517	3.805	2.767
V16	-1.433	0.785	1.078	3.814	0.316	3.819	0.464	3.818	2.827
V17	-1.581	0.796	1.104	3.811	0.321	3.817	0.470	3.817	2.838
V22	-1.414	0.827	1.089	3.812	0.328	3.816	0.478	3.815	2.837
V27	-1.489	0.781	1.079	3.814	0.314	3.820	0.462	3.819	2.836
V29	-1.489	0.795	1.077	3.814	0.314	3.820	0.461	3.819	2.842
V30	-1.303	0.790	1.068	3.815	0.321	3.818	0.471	3.816	2.815
V31	-1.368	0.815	1.060	3.816	0.318	3.820	0.467	3.817	2.845
Mean	-1.432±0.020	0.778±0.003	1.167±0.013	3.804±0.001	0.356±0.005	3.806±0.002	0.514±0.006	3.805±0.002	2.762±0.010

**Note.** — The properties in this table were calculated from the Fourier coefficients for the light curves using the equations described in Kuehn et al. (2011). The mean values were computed using only the first five stars, which have the lowest  $D_{max}$  values (Table 4).

**Table 7**  
Derived Physical Properties for RRc Variables

ID	$[\text{Fe}/\text{H}]_{\text{ZW84}}$	$\langle M_V \rangle$	$M/M_{\odot}$	$\log(L/L_{\odot})$	$\log T_{\text{eff}}$	Y
V10	-1.810	0.677	0.593	1.738	3.860	0.266
V25	-1.710	0.682	0.604	1.720	3.863	0.270
V28	-1.722	0.709	0.631	1.720	3.863	0.269
Mean	-1.747±0.032	0.689±0.010	0.609±0.011	1.726±0.006	3.862±0.001	0.268±0.001

**Table 8**  
Reddening from RRab Stars

ID	$(V - I)_{min}$	$E(V - I)$
V01	0.52	-0.06
V02	0.61	0.03
V05	0.59	0.01
V06	0.51	-0.07
V07	0.52	-0.06
V08	0.55	-0.03
V09	0.56	-0.02
V13	0.63	0.05
V14	0.58	0.00
V16	0.58	0.00
V17	0.54	-0.04
V18	0.59	0.01
V19	0.58	0.00
V20	0.57	-0.01
V21	0.57	-0.01
V22	0.59	0.01
V23	0.60	0.02
V26	0.60	0.02
V27	0.51	-0.07
V29	0.60	0.02
V30	0.61	0.03
V31	0.55	-0.03